Gene Expression, Vol. 11, pp. 181–197
Printed in the USA.

1052-2166/03 $20.00 + .00

Gene Expression Profiling of the Hypoxia Signaling Pathway in Hypoxia-Inducible Factor 1α Null Mouse Embryonic Fibroblasts

AJITH VENGELLUR,* BARBARA G. WOODS,* HEATHER E. RYAN,† RANDALL S. JOHNSON,† AND JOHN J. LAPRES*[1]

Department of Biochemistry and Molecular Biology and The National Food Safety and Toxicology Center, Michigan State University, East Lansing, MI 48824
†*Molecular Biology Section, Division of Biological Sciences, University of California, San Diego, CA 92093*

Hypoxia is defined as a deficiency of oxygen reaching the tissues of the body, and it plays a critical role in development and pathological conditions, such as cancer. Once tumors outgrow their blood supply, their central portion becomes hypoxic and the tumor stimulates angiogenesis through the activation of the hypoxia-inducible factors (HIFs). HIFs are transcription factors that are regulated in an oxygen-dependent manner by a group of prolyl hydroxylases (known as PHDs or HPHs). Our understanding of hypoxia signaling is limited by our incomplete knowledge of HIF target genes. cDNA microarrays and a cell line lacking a principal HIF protein, HIF1α, were used to identify a more complete set of hypoxia-regulated genes. The microarrays identified a group of 286 clones that were significantly influenced by hypoxia and 54 of these were coordinately regulated by cobalt chloride. The expression profile of HIF1α –/– cells also identified a group of downregulated genes encoding enzymes involved in protecting cells from oxidative stress, offering an explanation for the increased sensitivity of HIF1α –/– cells to agents that promote this type of response. The microarray studies confirmed the hypoxia-induced expression of the HIF regulating prolyl hydroxylase, PHD2. An analysis of the members of the PHD family revealed that they are differentially regulated by cobalt chloride and hypoxia. These results suggest that HIF1α is the predominant isoform in fibroblasts and that it regulates a wide battery of genes critical for normal cellular function and survival under various stresses.

Hypoxia cDNA microarray HIF1 protein Genomics Fibroblast

OVER 500,000 Americans will die of cancer this year. The progression of a single cell into a life-threatening tumor requires many steps. One of the steps in this progression is the ability of the tumor to escape the detrimental effects caused by hypoxia as it outgrows its blood supply. Hypoxia is defined as a state in which oxygen tension drops below the normal limits of 3.3–8% found in tissue beds (53). Hypoxia plays a central role in tumorigenesis but also has profound implications in normal cellular processes and development (46). Organisms have developed a programmed response to oxygen deprivation because of the critical role oxygen plays in energy production and survival (4). Central to an organism's response to hypoxia is the transcriptional upregulation of genes capable of stimulating glycolysis, angiogenesis, and erythropoiesis (33,36,47). Well-known and characterized hypoxia-regulated genes include erythropoietin (EPO), vascular endothelial growth factor (VEGF), platelet-derived growth factor (PDGF), and many others (11,12,30,45). Understanding hypoxia signaling, its transcriptional control, and a complete assessment of target genes is critical to our ability to influence this signaling cascade and thereby

Accepted September 22, 2003.
[1]Address correspondence to John J. LaPres, 402 Biochemistry Building, Michigan State University, East Lansing, MI 48824-1319. Tel: (517) 432-9282; Fax: (517) 353-9334; E-mail: lapres@msu.edu

treat or prevent illness that results in decreases in available oxygen.

Hypoxia-induced gene expression influences multiple processes within a tumor. As the tumor progresses past the 2-mm stage, cells within the central portion become hypoxic due to inadequate blood supply. This decrease in oxygen tension promotes angiogenesis through upregulation of growth factors such as VEGF and PDGF (5,11,13,37). In addition, cells exposed to hypoxia upregulate the expression of glycolytic enzymes to address their diminished capacity to produce ATP by oxidative phosphorylation. The final compensatory response is the upregulation of the growth factor EPO to stimulate the production of red blood cells. All of these responses are regulated by the hypoxia-inducible factors (HIFs).

The HIFs, which include HIF1α, HIF2α, HIF3α, ARNT (aryl hydrocarbon receptor nuclear translocator, also known as HIF1β), and ARNT2, control the cellular response to hypoxia (15). HIF1α, HIF2α, and HIF3α are primarily cytoplasmic and under normal oxygen tension are quickly degraded by a ubiquitin-mediated process. Their degradation is dependent upon protein motifs found in the carboxyl terminus of these proteins, termed hypoxia responsive domains (HRDs) (17). An HRD contains a proline residue that is modified by a recently described family of prolyl hydroxylases. These prolyl hydroxylases were first identified in *C. elegans* and were later shown to have three mammalian homologs (2,8). These prolyl hydroxylase domain-containing proteins (PHD 1, 2, and 3, also known as HPHs) are iron and 2-oxoglutarate dependent and use oxygen as a cosubstrate (2,44). Hydroxylation of the HIFs by the PHDs allows their interaction with the Von Hippel Lindau (VHL) tumor suppressor protein, which directs HIF degradation by recruiting the ubiquitination machinery. By contrast, under hypoxic conditions, the PHDs are unable to hydroxylate the cytoplasmic HIFs. The unmodified HIFs are stabilized and signaled by an unknown mechanism to translocate to the nucleus where they are free to form dimers with ARNT or ARNT2 (24,25). The HIF:ARNT heterodimers bind genomic DNA at sequence-specific sites termed hypoxia response elements (HREs) (50). In addition, HIF stability is also influenced by acetylation and its transcriptional activity is also regulated by hydroxylation (14,19,35).

The HIF1α:ARNT dimer is the most widely studied hypoxia signaling factor. HIF1α is critical for normal development and is essential for tumorigenesis (42,43). The HIF1α null animal is embryonic lethal due to vascularization defects, severely limiting its use in the study of HIF1α in vivo (43). Recently, a conditional null animal was created for HIF1α using the Cre-LoxP system (42). Subsequently, an immortal mouse embryonic fibroblast (MEF) cell line was established from this mouse model (42). The conditional animal and cell line make it possible to understand the role of HIF1α in vivo at various developmental time points, tissues, and under various conditions.

The identification of the PHD family of enzymes has increased our understanding of the upstream events leading to HIF-mediated transcription. The library of hypoxia-regulated genes, though extensive, remains incomplete. Our understanding of the hypoxia signaling system is dependent upon a thorough characterization of genes influenced by hypoxia signaling, both directly and indirectly. Here we have used cDNA microarrays and the HIF1α null MEF cell line to begin to fill this knowledge gap. Our results demonstrate that HIF1α is the primary mediator of hypoxia signaling in MEFs. The microarray experiments have detailed several groups of HIF1α-dependent genes. Among these HIF1α-dependent genes are the glycolytic enzymes and several proapoptotic factors. Most have been previously identified as hypoxia regulated; however, some of these had not been previously characterized as HIF-driven genes. Among the novel HIF1α-dependent genes identified in the microarray experiments and confirmed by relative real-time PCR (rRT-PCR) was PHD2. In addition, PHD3 also showed HIF1α-dependent regulation. Overexpression of the PHDs was also shown to lead to a decrease in hypoxia-induced gene transcription. The microarray study also gave some insight into the role of HIF1α in cellular homeostasis. The direct comparison of untreated wild-type and HIF1α –/– cells identified a group of genes influenced by the loss of the HIF1α protein. These included genes that encode for proteins involved in protection against oxidative stress. These results suggest that the HIF1α protein regulates a wide variety of genes and may be partially regulated by feedback inhibition.

MATERIALS AND METHODS

Materials

Tissue culture media, supplements, and fetal bovine serum were obtained from Invitrogen, Inc. (Carlsbad, CA). The synthesis of oligonucleotides was performed by the macromolecular facility, Michigan State University, East Lansing, MI. SYBR Green Dye and 6-carboxy-X-rhodamine were purchased from Molecular Probes (Eugene, OR). AmpliTaq™ Gold PCR buffer and AmpliTaqTM Gold DNA polymerase were purchased from Perkin-Elmer (Wellesley, MA). All other chemicals were reagent grade and obtained from Sigma-Aldrich Chemicals (St. Louis, MO).

Cell Culture, Nuclear Extracts, and Western Blotting

Mouse embryonic fibroblast cell lines were maintained in DMEM medium [10% heat-inactivated FBS, penicillin-streptomycin (10 U/ml), nonessential amino acid (10 μg/ml), L-glutamine (2 mM)] and grown at 37°C in 5% CO_2. Hypoxia treatments were performed in an oxygen-regulated incubator (Precision, Winchester, VA) or simulated by treating the cells with 100 μM of $CoCl_2$ (dissolved in H_2O).

Wild-type and HIF1α –/– cells were grown under normoxic (20% O_2) or hypoxic (1% O_2) conditions or in the presence of 100 μM $CoCl_2$ for 6 h. Nuclear extracts were prepared as described previously with minor modifications (20). Briefly, cells were washed with cold PBS (4°C) and removed from the surface by scraping in cell lysis buffer (10 mM Tris-HCl, pH 8.0, 1 mM EDTA, 150 mM NaCl, 1 μg/ml each of aprotinin, leupeptin, pepstatin A, and 1 mM PMSF) and homogenized. The nuclei were removed by centrifugation (4000 rpm, 15 min) and the supernatant was saved. The nuclei were lysed upon addition of nuclei lysis buffer (20 mM HEPES, pH 7.9, 400 mM NaCl, 1 mM EDTA, and 1 mM DTT, 1 μg/ml each of aprotinin, leupeptin, pepstatin A, and 1 mM PMSF). Insoluble matter was removed by centrifugation ($10{,}000 \times g$, 15 min). The protein concentration of the supernatant was determined by standard colorimetric assay via the manufacturer's instructions (Bio-Rad, Hercules, CA). Equal amounts of protein for each sample were separated by SDS-PAGE, and Western blotting was performed with a HIF1α-specific antibody (Novus Biologicals, Littleton, CO). A horseradish peroxidase-conjugated secondary antibody was used to facilitate detection. The blot was stripped and reprobed with a β-actin-specific antibody (a generous gift from Dr. John Wang, Michigan State University). The blots were exposed using a chemiluminescent assay kit (Amersham Biosciences, Piscataway, NJ).

cDNA Microarray Production

The National Institute of Aging 15K clone set was used for the production of the microarray (26,52). The NIA 15K set was supplemented with an additional 96 clones to bring the total number of clones to 15,360. Each clone was PCR amplified with modified M13 forward and reverse primers (Table 1). Each primer was modified on the 5′ end with an amino linker to facilitate linkage to the aldehyde-modified glass substrate. Amplicons were precipitated and the size and quality verified by agarose gel electrophoresis, then resuspended in 3× SSC. The full 15K set was printed on Telechem™ Superaldehyde slides (Telechem International Inc., Sunnyvale, CA) using an OmniGrid™ robot (GenMachines®, San Carlos, CA) with Chipmaker 2 microarray pins (Telechem International Inc).

Microarray Experimental Design

The microarray experiments were performed using a "loop" design (27) (Fig. 1). This design was chosen to increase the statistical strength of the model, to allow for effective comparison between treatments and cell types and to facilitate the long-term goals of the project. Total RNA from two independent 10-cm tissue culture plates (approximately 1×10^7 cells) within each treatment were labeled. Each RNA sample was labeled four times, twice with Cy3 and twice with Cy5. Two complete loops were performed; therefore, four independent cultures were labeled twice, once with each dye, equaling a total of eight individual labeling reactions per treatment group. It is important to note that the loop design does not utilize the calculation of expression intensity ratios but relies on the averaged expression within each treatment over all of the labeling reactions (in this case eight). Expression patterns are then statistically analyzed to determine those genes for which expression is significantly changed (below). Ratios can be calculated for each treatment by direct comparison of the averaged expression between the treatments of interest.

RNA Extraction and cDNA Microarray Probe Labeling and Hybridization

RNA extraction was performed using Trizol reagent (Invitrogen) via the manufacturer's instructions and quantitated spectrophotometrically. Total RNA (30 μg) from wild-type or HIF1α –/– cells grown for 24 h under normoxic (20% O_2) or hypoxic (1% O_2) conditions or in the presence of 100 μM $CoCl_2$ was used to generate probes as follows. Total RNA was incubated with 6 μg anchored oligo-dT primers (5′-T_{21}VN-3′). The reverse transcription was performed using Superscript™ II RNase H-Reverse Transcriptase (400 U, Invitrogen) in the presence of aminoallyl dUTP (aa-dUTP) (Amersham Biosciences, Piscataway, NJ), dTTP, dATP, dCTP, and dGTP (final dNTPs = 0.5 mM). The ratio of aa-dUTP to dTTP was 2:1. The unincorporated nucleotides were removed using the QIAquick™ PCR purification kit (Qiagen Inc., Valencia, CA) according to the manufacturer's instructions, after substituting the wash buffer with phosphate wash buffer (5 mM KPO_4, pH 8.0, in 80% ethanol), and eluted with 4 mM KPO_4 (pH 8.5). The probes were dried under vacuum centrifugation and resuspended in 0.1 M Na_2CO_3 (pH 9.0) and conjugated to monoreactive Cy3 and Cy5 dyes (Amersham Biosciences). Unincorporated dyes

TABLE 1
PRIMERS FOR MICROARRAY PRODUCTION AND RT-PCR

Gene	Accession #	Forward	Reverse
M13		CTGCAAGGCGATTAAGTTGGGTAAC	CTGCAAGGCGATTAAGTTGGGTAAC
HPRT	NM_013556	AAGCCTAAGATGAGCGCAAG	TTACTAGGCAGATGGCCACA
GAPDH	M32599	ACCCAGAAGACTGTGGATGG	TTCAGCTCTGGGATGACCTT
P4H	NM_011031	CTGTTGTGGCCCGAGTAAAT	GAAGTCGAAGTGCGGTTCAT
PHD1	AF453879	GGAACCCACATGAGGTGAAG	AACACCTTTCTGTCCCGATG
PHD2	XM_134453	GAAGCTGGGCAACTACAGGA	CATGTCACGCATCTTCCATC
PHD3	NM_028133	AAGTTACACGGAGGGGTCCT	GGCTGGACTTCATGTGGATT
SOD1	BC002066	GAGACCTGGGCAATGTGACT	TTGTTTCTCATGGACCACCA
SOD2	BC018173	AACTCAGGTCGCTCTTCAGC	GCTTGATAGCCTCCAGCAAC
Catalase	NM_009804	CCAGTTGGCAAAGTGGTTTT	GCCCTGAAGCTTTTTGTCAG
GST-μ	NM_0010358	CACAAGATCACCCAGAGCAA	GGTGTCCATGACCTGGTTCT

were removed using the QIAquick™ nucleotide removal kit (Qiagen Inc.). Microarrays were prehybridized in pre-hyb buffer (5× SSC, 0.1% w/v SDS, 1% w/v BSA) for 2 h at 42°C. Cy3- and Cy5-labeled probes were resuspended in hybridization buffer [50% formamide, 5× SSC, 0.1% SDS, 2 μg Cot1 DNA, and 20 μg poly(A)-DNA] and denatured at 95°C for 3 min. The probes were hybridized for at least 20 h to the microarrays at 42°C under Lifter slips™ (Erie Scientific Company, Portsmouth, NH). Slides were washed as follows: 1) brief wash with 1× SSC and 0.2% SDS at 42°C to remove the coverslips; 2) 4 min in 1× SSC and 0.2% SDS at 42°C; 3) 4 min in 0.1× SSC and 0.2% SDS at room temperature; and 4) twice for 2.5 min each in 0.1× SSC at room temperature. Slides were dried and scanned immediately.

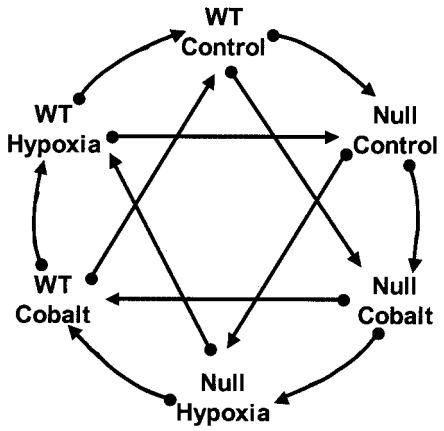

Figure 1. Experimental design of loop. Graphical representation of the 2V loop experimental design. Each arrow represents a single microarray slide. The arrowhead represents the sample labeled with Cy5 and the arrow tail represents sample labeled with Cy3. Because the loop was performed twice, each treatment group sample was labeled in eight separate reactions, four with Cy3 and four with Cy5.

Microarray Data Analysis

Slides were scanned with an Affymetrix™ 428 scanner (Affymetrix, Santa Clara, CA) at 532 nm (Cy3) and 635 nm (Cy5). The images were analyzed using GenePix™ Version 3.0 software (Axon Instruments Inc., Union City, CA) and output files were analyzed using GP3 (http://www.bch.msu.edu/~zacharet/microarray/gp3.html) (10). GP3 automatically flags spots with intensities below background levels, corrects for background signal, and normalizes the two channels using a *z*-score method. The GP3 output values were normalized within the loop using the Centralizer program (57) (http://cartan.gmd.de/~zien/centralization/). Genes differentially expressed between treatments were identified by *t*-test (two-tailed, unequal variance, $p \leq 0.05$ cutoff). All genes called present [signal > (background + 2 SD of background)] were hierarchically clustered using GeneSpring™, v 4.2.1 (Silicon Genetics, Redwood City, CA).

Relative Real-Time PCR Analysis

Changes in gene expression observed by microarray analyses were verified by real-time PCR, performed on an Applied Biosystems Prism 7000 Sequence detection System (Foster City, CA). To synthesize cDNA, total RNA (1 μg per sample per treatment, $n = 6$) was used as template for a reverse transcriptase reaction in 20 μl of 1× First Strand Synthesis buffer (Invitrogen) containing 1 μg oligo (5′-T_{21}VN-3′), 0.2 mM dNTPs, 10 mM DTT, and 200 IU of Superscript II reverse transcriptase (Invitrogen). The reaction mixture was incubated at 42°C for 60 min, and stopped by incubation at 75°C for 15 min. Amplification of cDNA (1/20) was performed using SYBR Green PCR buffer [1× AmpliTaq™ Gold PCR Buffer, 0.025 U/μl AmpliTaq™ Gold (Perkin-Elmer), 0.2 mM dNTPs, 1 ng/μl 6-carboxy-X-rhodamine, 1:40,000

diluted SYBR® Green Dye, and 3% DMSO] and 0.1 μM primers. The thermal cycling parameters were 95°C for 10 min followed by 40 cycles of 95°C for 15 s and 60°C for 60 s. The relative abundance of the mRNA was normalized to hypoxanthine-guanine phosphoribosyl transferase message. Each primer set produced a single product as determined by melt-curve analysis. *t*-Tests were performed between treated and control samples within each cell type using the statistical package, SAS v8.2.

Primers were designed using the Web-based application Primer3 (http://www-genome.wi.mit.edu/cgi-bin/primer/primer3_www.cgi) biasing towards the 3′ end of the transcript to maximize the likelihood of giving a gene-specific product. The settings used in Primer3 were 125 bp amplicon, 20mer, 60°C melting temperatures, and all other as defaults. Gene names, accession numbers, and forward and reverse primer sequences are listed in Table 1.

Transient Transfection of Hep3B Cells

Hep3B cells were maintained in DMEM + 5% FBS (growth medium). Prior to transfection, cells were washed twice with serum-free medium (DMEM). Cells were transfected using Lipofectamine (LF) (Invitrogen) via the manufacturer's instructions using 5 μl of LF with an incubation time of 6 h prior to addition of growth medium. Cells were transfected with an HRE-driven luciferase reporter, a β-galactosidase (β-GAL) expression vector for control of transfection efficiency, and the various PHD expression vectors (a generous gift of Dr. Peter Ratcliff, University of Oxford, UK). All transfections were normalized for DNA content with an empty expression vector. DNA was incubated with rehydrated LF for 15 min prior to transfection. Cells were then treated with DNA/LF mix for 6 h. Following this, incubation medium was removed and replaced with growth medium and placed into normoxia (20% O_2) or hypoxia (1% O_2) incubator. Cells were incubated for 18 h and assayed for luciferase and β-Gal activity via standard assays (Promega, Madison, WI). Luciferase values were normalized to β-Gal activity in each well and untreated empty expression vector within experiments.

RESULTS

Verification of the MEF Cell Line Phenotype

A Western blot was performed on the cell lines used in our microarray experiments to verify their phenotype. Wild-type and HIF1α –/– cells were exposed to $CoCl_2$ (100 μM) or hypoxia (1% O_2) for 6 h. Nuclear extracts were prepared from treated and untreated cells and analyzed using a HIF1α-specific antibody (Novus Biologicals, Littleton, CO). As expected, HIF1α was only detectable in the wild-type cells. A very small amount was observed in untreated cells but greatly increased following exposure to cobalt or hypoxia (Fig. 2). There was also a migratory shift in these treated fractions, suggesting a protein modification. The blot was reprobed with an antibody specific to β-actin to verify loading (Fig. 2).

Hierarchical Cluster Analysis of Microarray Data

cDNA microarrays have given researchers an opportunity to understand signaling networks as they relate to global changes in gene expression. Here microarrays were used to characterize hypoxia signaling and the role of HIF1α in this process. Two cell lines were used: the wild-type and the HIF1α –/– MEFs. Each cell line was left untreated (control, 20% O_2) or treated with hypoxia (1% O_2) or cobalt chloride (100 μM) for 24 h. Cobalt has been extensively used as a hypoxia mimic and has been shown to inhibit the activity of the PHDs (8). The microarray experiments were performed in a "loop" design as described above (Fig. 1) and statistically analyzed (28).

Hierarchical cluster analysis of microarray data along treatments and genes creates relationships between groups based on expression patterns observed in the gene set as a whole. Here we used cluster analysis to identify combinations of treatments and genotype that were similar at the gene expression level and to identify groups of genes responding in a similar manner among the various treatment and genotype combinations. As expected, results from $CoCl_2$ and hypoxia treatments in the wild-type cells clustered together (Fig. 3). This similarity in gene expression between these two treatments did not extend to the null MEFs. These results suggest that $CoCl_2$ and hypoxia

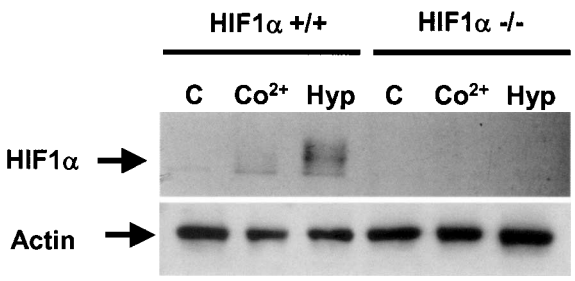

Figure 2. HIF1α Western blot. Wild-type (HIF1α +/+) and null (HIF1α –/–) cells were exposed to $CoCl_2$ (Co^{2+}, 100 μM) or hypoxia (Hyp, 1% O_2) for 6 h or left untreated (C). Nuclear extracts were prepared and proteins were separated by SDS-PAGE, transferred to nitrocellulose membrane, and probed with a HIF1α-specific antibody (upper panel). Blot was reprobed with β-actin to verify equal loading (lower panel).

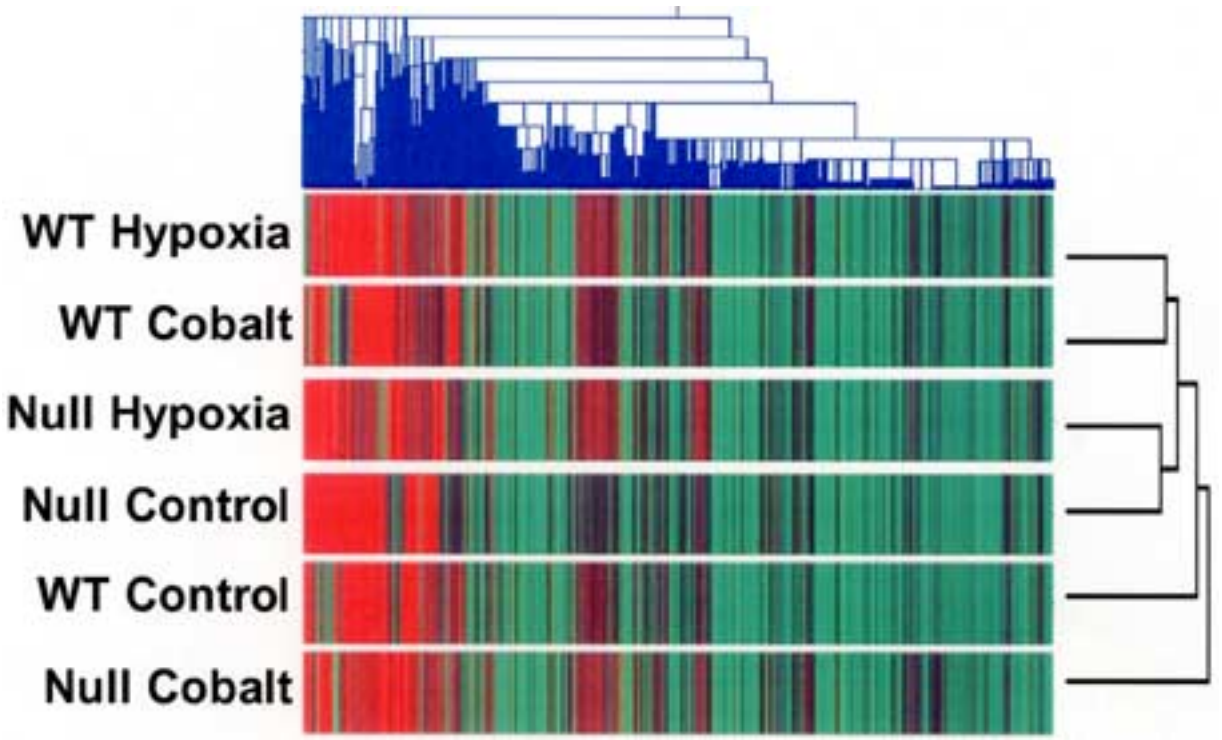

Figure 3. Hierarchical cluster diagram of entire data set. The microarray data were filtered to remove genes for which expression was determined to be insignificant [signal < (background + 2 SD background)]. Expression results from the filtered data were clustered by treatment and gene. The relationships are represented as a dendrogram in both directions. Red represents a high level of expression and green represents low expression.

are driving expression of a similar gene cluster and that HIF1α is essential for this regulation. Interestingly, the HIF1α –/– cells under hypoxic conditions behaved most like the null control cells (Fig. 3). The loss of hypoxia signaling and comparable expression pattern between hypoxia and control suggests that HIF1α is central to hypoxia-mediated signaling in these cells.

Statistical Comparison of Hypoxia and Cobalt Treatment in WT Cells

The major focus of these microarray studies was to identify a more complete battery of hypoxia-regulated genes. This was accomplished first by statistical assessment of expression patterns within the data. Stringent criteria were set to minimize the possibility of false positives. First, the results from wild-type cells were screened for all genes whose expression was significantly altered by treatment ($p < 0.05$ compared with untreated control). The results show that expression of 286 clones was significantly ($p \leq 0.05$) altered by hypoxia and 252 were altered by cobalt (Fig. 4). A complete list of the genes significantly altered by hypoxia or cobalt can be found at: http://www.bch.msu.edu/lapres/SupplementalData_total.pdf (supplemental data Table D and E). Next, we determined the overlap within these two sets and found that there were 54 clones representing 49 different genes that were in both of these groups. These 54 clones were then analyzed for gene ontology information and grouped accordingly (Table 2). Finally, we determined how many of these genes were also altered in the HIF1α –/– cells under the same conditions. None of these 49 genes were altered in both hypoxia and cobalt in the null cells. However, 7 of the 49 genes in Table 2 were significantly altered in the HIF1α –/– cells in either cobalt or hypoxia treatment. The genes for metallothionein (clone A-2031) and transglutaminase (clone H3137C06) were influenced in the HIF1α –/– cells by cobalt. The HIF1α-independent increase in metallothionein is most likely due to its regulation by the metal transcription factor (39). Five of the 49 genes were shown to be significantly influenced by hypoxia in the null cells. These genes were pyruvate kinase 3 (clones H3030D10 and H3030D11), cathepsin L (clone H3028F03), galectin 3 (clone H3016D10), tissue-specific transplantation antigen P35B (clone H3147H11), and one gene with unknown function (clone H3116A06). It should be noted that the pyruvate kinase 3 gene was significantly downregulated in the null cells while being

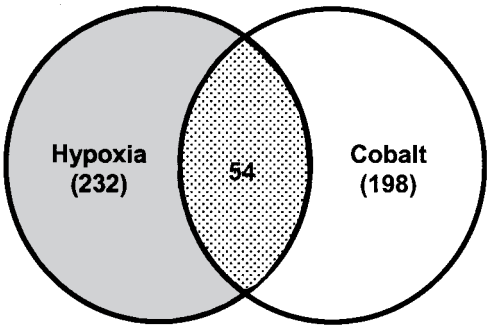

Figure 4. Analysis of $CoCl_2$ and hypoxia treatment in wild-type cells. The Venn diagram represents total number of genes unique to each treatment group (in parentheses) and the number of genes shared between the two treatments. A complete list of genes in both treatment groups can be found at: http://www.bch.msu.edu/lapres/SupplementalData_total.pdf (supplemental data Tables D and E).

significantly upregulated in the wild-type cells under hypoxia. These results suggest that the changes in expression patterns for the transcripts represented within Figure 4 are predominantly HIF1α dependent.

Only 12 of the 49 genes in Figure 4 and Table 2 had been previously associated with hypoxia signaling. The 54 clones were separated into seven categories by ontology. The largest group that could be assigned a function consists of glycolytic enzymes (11 clones, 7 genes, Table 2). These enzymes are well-known targets of the hypoxia signaling cascade. There were several genes in other groups that also had been identified as hypoxia targets. Most notable are proline-4-hydroxylase (P4Ha2, clone H3003D12) and BCL2/adenovirus E1B 19 kDa-interacting protein 3-like (BNIP3L or NIX, clone H3016D08). There were also several groups that had not been previously identified as hypoxia targets. These include a large group of matrix remodeling genes and cellular antigens. The largest group was comprised of clones for which function has not yet been assigned (Table 2).

Comparison of Hypoxia and Cobalt Treatment in HIF1α –/– Cells

As noted above, only a handful of genes identified in Figure 4 and Table 2 were significantly changed in null cells. None of these genes (metallothionein, pyruvate kinase, transglutaminase, cathepsin L, and galectin 3) were influenced in both treatments in the null cells. To further clarify the HIF1α independently regulated genes from the microarray studies, a comparison between cobalt- and hypoxia-treated HIF1α –/– cells was performed. There were 376 clones significantly altered in these cells upon exposure to hypoxia (1%, 24 h) and 349 clones significantly altered upon exposure to cobalt (100 μM, 24 h) (supplemental data Table F and G). There were 65 clones that were shared between these two lists (Fig. 5A). Of these 65 clones, none were found in the list for the wild-type cells (Table 2, supplemental data Table A). These 65 clones represented several different enzymes including subunits of ATPase and biliverdin reductase B (BLRVB). BLRVB is downstream of heme oxygenase 1 in the metabolism of heme. Heme oxygenase, a known hypoxia-regulated gene, converts heme into carbon monoxide, biliverdin, and free iron. BLRVB converts biliverdin into bilirubin (7,32, 56). This suggests that the pathway for heme degradation is not coordinately regulated under hypoxic conditions. This group also contained a receptor for tumor necrosis factor and raises the possibility that hypoxia and hypoxic mimics influence the expression of the receptor of a factor known to play a role in hypoxia signaling (22,31). These 65 clones presumably represent a subset of genes that can be influenced by hypoxia and cobalt in a HIF1α-independent manner and may involve HIF2α or HIF3α because both are expressed in these cells at a much lower level than that of HIF1α (data not shown).

Comparison of Hypoxia Treatment in Wild-Type and HIF1α –/– Cells

The comparisons described in Figures 4 and 5A were done using those genes that were significantly changed by hypoxia and cobalt. To identify genes regulated in a HIF1α-independent manner by hypoxia alone, a comparison between hypoxia treatments in wild-type and HIF1α –/– cells was performed. There were 26 genes that were significantly influenced by hypoxia in both cell types (Fig. 5B, supplemental data Table B). These genes included those described above (Fig. 4, Table 2), as well as procollagen. Hypoxia-induced collagen synthesis has been previously described and may be critical to several disease states (9,49). Interestingly, procollagen is upregulated in the wild-type cells and downregulated in the HIF1α –/– cells upon exposure to hypoxia, similar to the pyruvate kinase 3 gene mentioned above.

Comparison of Cobalt Treatment in Wild-Type and HIF1α –/– Cells

A comparison between wild-type and HIF1α –/– cells was also performed for genes significantly influenced by cobalt. Though cobalt is used as a hypoxia mimic, there is no overlap between the 14 genes identified in this comparison and those found for the hypoxia comparison (Fig. 5B and C, supplemental data

TABLE 2
SIGNIFICANTLY INFLUENCED GENES IN WT CELLS TREATED WITH HYPOXIA AND COBALT

ID	Gene Name	Abbr.	Fold Changes W-Co	W-H	N-Co	N-H
Extracellular (GO = 0005615, 0005576, 0005578)						
H3003D12	proline 4-hydroxylase	P4ha2	1.29	2.61	0.97	1.05
H3011E02	chorionic somatomammotropin hormone 1	Csh1	0.67	0.80	0.81	0.82
H3027D05	lymphocyte antigen 6 complex, locus E	Ly6e	0.78	1.26	0.88	0.84
H3028F03	cathepsin L	Ctsl	2.17	1.54	1.28	2.92
H3058D07	matrix metalloproteinase 23	Mmp23	0.71	1.43	0.49	0.55
H3109A05	CD24a antigen	Cd24a	0.71	0.67	0.59	0.62
H3115F11	nidogen-2	Nid2	1.40	1.35	0.76	1.05
Mitochondrial (GO = 0005762, 0005739, 0005743)						
H3016D08	BCL2/adenovirus E1B 19kDa-interacting protein 3-like	Bnip3l	1.39	1.58	0.91	0.95
H3029D09	mitochondrial ribosomal protein S11	Mrps11	0.81	0.77	1.40	0.86
H3052D11	adenylate kinase 2	Ak2	0.74	0.74	0.93	0.96
H3137G05	mitochondrial ribosomal protein L17	Mrpl17	0.55	0.60	1.03	0.77
H3143D12	mitochondrial carrier homolog 1 (*C. elegans*)	Mtch1	1.45	1.55	1.05	1.21
Glycolytic Enzymes (GO = 0006096)						
H3012A11	glyceraldehyde-3-phosphate dehydrogenase	Gapd	1.36	1.63	0.79	0.82
H3019E08	glyceraldehyde-3-phosphate dehydrogenase	Gapd	1.45	1.75	0.90	0.86
H3023D06	phosphoglycerate kinase 1	Pgk1	2.31	3.67	0.69	0.93
H3023H12	lactate dehydrogenase 1, A chain	Ldh1	2.71	3.93	0.86	0.89
H3027E07	enolase 1, alpha nonneuron	Eno1	1.94	1.82	0.75	0.92
H3027E08	enolase 1, alpha nonneuron	Eno1	2.12	3.02	0.98	1.10
H3027E09	enolase 1, alpha nonneuron	Eno1	1.76	2.48	0.87	0.75
H3030D10	pyruvate kinase, muscle	Pkm2	1.62	2.02	0.86	0.69
H3030D11	pyruvate kinase, muscle	Pkm2	1.93	2.36	0.87	0.65
H3031D03	aldolase 1, A isoform	Aldo1	1.35	1.92	0.88	0.92
H3149C10	triosephosphate isomerase	Tpi	2.06	2.18	0.82	0.81
Membrane Proteins (GO = 0016021)						
H3022E01	membrane bound C2 domain containing protein	Mbc2	1.24	1.22	1.01	1.04
H3151C09	CD 81 antigen	Cd81	1.49	1.44	0.96	1.25
Enzymes and Misc Function (Various GO)						
H3016D10	lectin, galactose binding, soluble 3	lgal3	1.46	1.62	1.07	1.32
H3016G08	cask-interacting protein 2	Caskin2	1.64	1.82	1.17	1.28
H3019C07	macrophage migration inhibitory factor	Mif	1.69	1.95	1.21	1.05
H3020C02	metallothionein 1	Mt1	2.07	1.27	1.25	1.11
A-2031	metallothionein 1 (image 1052401)	Mt1	2.810	1.784	2.134	1.561
H3031B12	minichromosome main. Def. 3 assoc. protein	Mcm3ap	1.42	1.33	0.92	0.96
H3137C06	transglutaminase 2, C polypeptide	Tgm2	0.63	0.85	0.56	0.88
H3147H11	tissue specific transplantation antigen P35B	Tsta3	1.73	1.47	1.26	1.45
H3016F05	similar to translation initiation factor 3, subunit 4	Eif3s4	0.89	0.83	0.99	0.91
H3130A05	proteasome 26S subunit, non-ATPase, 2	Psmd2	0.50	0.51	0.60	0.57
Function Unknown (Various GO)						
H3044B11	DNA segment, Chr 8		0.80	0.63	0.98	0.94
H3065C11	expressed sequence AU022848		0.61	0.70	0.80	0.90
H3118D07	DNA segment, Chr 11		0.77	0.90	1.01	0.97
H3128G06	expressed sequence AW215868		1.47	1.70	1.09	1.22
H3134C05	hypothetical protein LOC223886		0.67	0.54	0.71	0.53
H3142E06	RIKEN cDNA 1110031E24 gene		0.74	0.90	0.83	1.13
H3148A03	DNA segment, Chr 10		0.76	0.67	0.86	0.88
H3030G02	neurophilin-like molecule		1.77	2.20	1.12	1.12
H3108H01	human from clone RP11-494N1 on chromosome 9		0.80	0.73	1.08	0.99
H3116A06	*Mus musculus*, clone IMAGE:4024675, mRNA		1.24	1.35	1.08	1.30
H3132E05	mouse from clone RP23-170G19 on chromosome X		1.31	0.79	0.87	0.81
Unknown (Various GO)						
H3017G08			1.59	2.05	0.93	0.96
H3150A01			1.36	1.73	0.88	1.00
H3022E07			1.43	1.94	0.79	0.82
H3125B04			1.64	1.76	1.15	1.23
H3017D11			0.74	0.63	0.88	0.92
H3072E04			1.21	0.85	0.88	1.06
H3123A12			1.95	2.07	0.78	0.95
H3146H09			0.74	0.57	0.90	1.05

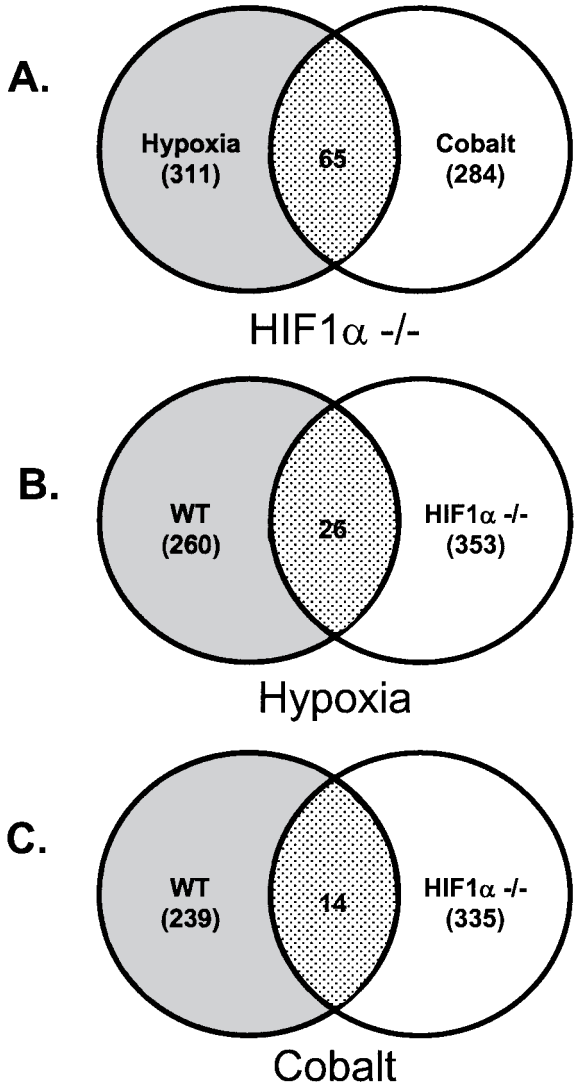

Figure 5. Venn diagrams of various combinations of cell types and treatments. Total number of genes unique to each treatment group (in parentheses) and the number of genes shared between the two treatments (central shaded area). (A) The Venn diagram representing genes significantly influenced by hypoxia and/or cobalt in HIF1α –/– cells. (B) Comparison of wild-type (WT) and HIF1α –/– cells following hypoxia treatment (1% O_2, 24 h). (C) Comparison of WT and HIF1α –/– cells following cobalt treatments (100 μM, 24 h). A complete list of genes in both treatment groups can be found at: http://www.bch.msu.edu/lapres/SupplementalData_total.pdf (supplemental data, Tables D–G).

Table C). The 14 genes in this list include metallothionein and transglutaminase 2 (Tg2). Tg2 was previously identified as a VHL/hypoxia target gene (55).

Comparison of Wild-Type ctrl and HIF1α –/– ctrl Cells

Finally, a direct comparison between untreated wild-type and HIF1α –/– cells was performed to determine the role of HIF1α in cellular homeostasis. There were 234 genes influenced by the loss of HIF1α (supplemental data Table H). Of these, H19 was significantly upregulated by the loss of the HIF protein. The three clones, H3144B07, H3144B06, H3140G12, displayed a wild-type ctrl/HIF1α –/– ctrl ratio of 0.067, 0.211, and 0.131, respectively (average ninefold higher in HIF1α –/– cells). H19 is an imprinted gene involved in development and not highly expressed following birth (41). The reason for its aberrant expression following loss of the HIF1α protein is unknown. Another group of genes also stood out in this comparison of ctrl cells. The HIF1α –/– cells displayed a decreased expression level of genes involved in the cellular response to oxidative stress. These genes include glutathione *S*-transferase-μ (GST-μ, clones H3134F05, H3119G08, H3159G05), superoxide dismutase 1 (SOD1, clones H3130B11, H3130B11), SOD2 (A-2062), and catalase (A-2049) (supplemental data). This decreased level of these protective genes may explain why HIF1α –/– cells are more sensitive to oxidative stress (54). In addition, this decrease adds to the growing evidence of the complex role hypoxia signaling plays in normal cellular homeostasis and tumorigenesis.

The Glycolytic Cluster

One hypothesis of expression profiling is that genes that cluster together are regulated in a similar manner. We wanted to identify novel genes that may also play a role in the cellular response to hypoxia, and our hypothesis was that they would behave similarly, at the expression level, to the glycolytic enzymes. The glycolytic enzymes are critical to a cell's response to low oxygen tension and are direct targets of HIF-regulated transcription. We isolated a cluster of glycolytic genes from our microarray data and looked for functional information for several of the nonglycolytic genes (Fig. 6). First, three genes involved in apoptosis were found within this cluster. Two are known (BNIP3 and NIX) and one is a novel (PS receptor) hypoxia-regulated gene (3,48). The role that these genes play in the downstream events following acute and chronic hypoxia is currently being investigated.

Second, there were two hydroxylases identified within this glycolytic cluster (Fig. 6). The first, P4-H, is a procollagen prolyl 4-hydroxylase and a known hypoxia-regulated gene (51). It functions in a similar manner to that of the PHDs; however, it is unable to influence HIF stability in *C. elegans* (8). The second is EGL-9 homologue 1, also known as PHD2. As mentioned earlier, the PHDs negatively influence HIF signaling by controlling HIF stability. This result confirms previously published data and supports the

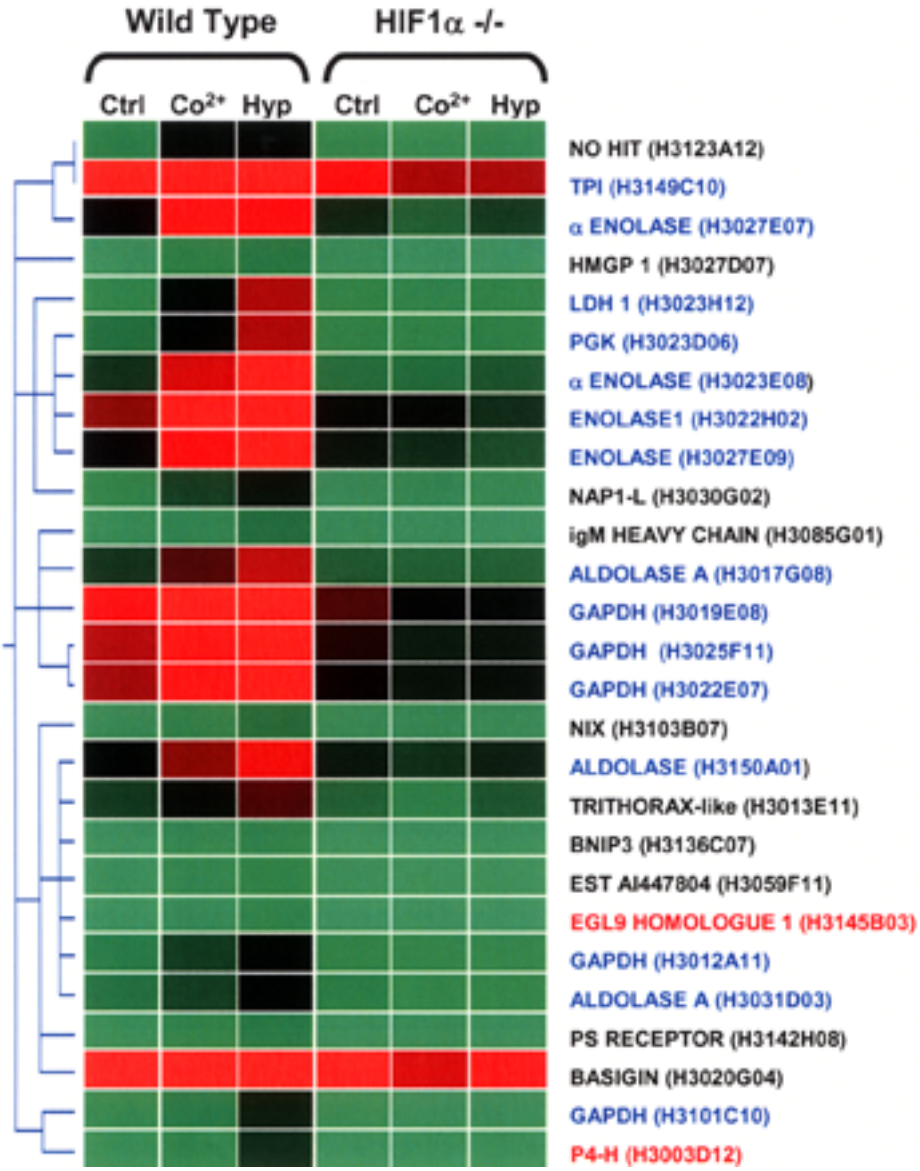

Figure 6. Glycolytic enzyme cluster. The cluster of glycolytic enzyme genes (Fig. 4) was further analyzed to identify novel hypoxia-regulated genes. Four subsets of genes were identified; the glycolytic enzyme genes (blue), apoptotic genes (green), hydroxylases (red), and others (black). Red represents a high level of expression and green represents low expression.

hypothesis that HIF1α may be partially controlled by feedback inhibition (1,8). It should be pointed out that PHD2 was not listed in Table 2 (genes altered by cobalt and hypoxia in wild-type cells) because the increase seen following cobalt exposure for this clone did not pass statistical cutoff (Fig. 7, supplemental data Table D).

Relative Real-Time PCR

We verified our microarray data by rRT-PCR using SYBR® Green as a fluorescent marker. The glycolytic enzyme glyceraldehyde-3-phosphate dehydrogenase (GAPDH) is a known hypoxia-regulated gene and acted as a positive control for our SYBR® Green protocol. GAPDH was also present on the microarray and shown to be regulated in a HIF1α-dependent manner (Figs. 4, 6, and 7A). In addition, the loss of GAPDH regulation by hypoxia in the HIF1α –/– suggests that HIF1α is the primary mediator of hypoxia signaling in MEFs. These results were confirmed in the rRT-PCR. Six separate biological samples were analyzed for each separate treatment in the two cell lines. There was a significant increase in GAPDH message in the cobalt- and hypoxia-treated wild-type cells when compared with the control. This increase

did not extend to the HIF1α –/– cell line (Fig. 7B). A similar HIF1α-dependent expression pattern was seen on the microarray for P4-H (Figs. 6 and 7C). This result was also verified on the rRT-PCR (Fig. 7D). The results for the cobalt treatment were not as pronounced as that following hypoxia exposure, though both were statistically significant. Finally, the expression pattern of PHD2 was also confirmed by rRT-PCR (Fig. 7E and F). There was only a modest increase in expression when the microarray was analyzed. The expression pattern among the treatment groups, however, was identical to that of other known hypoxia-regulated genes in the cluster (i.e., increased in cobalt and hypoxia in wild-type cells, no change in HIF1α –/– cells). The rRT-PCR results confirmed that PHD2 transcription increased in response to cobalt (>threefold) and hypoxia (>sixfold) when compared with the control treatment only in the wild-type cells. These results suggest that HIF1α may indirectly control its own stability by affecting the level of the prolyl hydroxylase that marks it for degradation. These data also shows the level of data compression that is often seen in microarray data due to normalization and other mathematical manipulation necessary for comparisons between multiple experiments and labelings (29). The difference in fold change in the microarray data is consistently underestimated. The relative compression of the data for var-

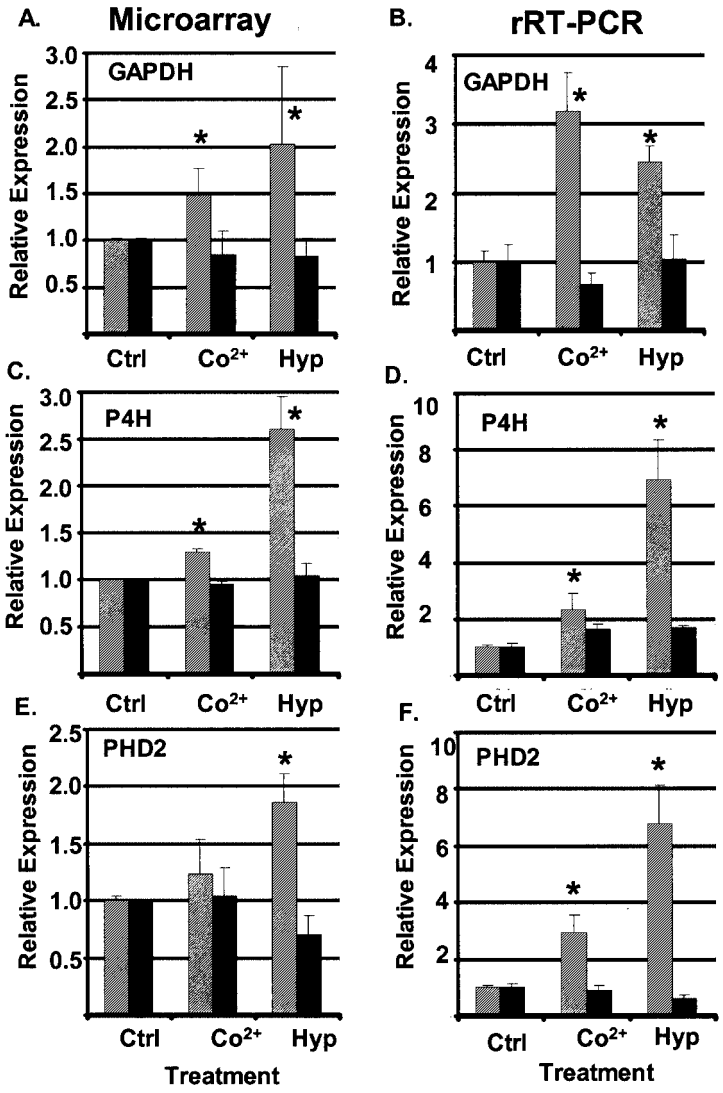

Figure 7. Comparison of microarray and rRT-PCR results. GAPDH (A, B), P4H (C, D), and PHD2 (E, F) were analyzed for expression levels in wild-type (hatched bars) and HIF1α –/– cells (solid bars) by microarray (A, C, E) and rRT-PCR (B, D, F) protocols. Each value was normalized to the control level in the corresponding cell line. Ctrl: untreated; Co^{2+}: 100 μM $CoCl_2$; Hyp: 1% O_2 for 24 h. Averaged expression within each treatment group was used to generate ratios (see experimental design). *$p < 0.05$ when compared with corresponding control.

ious genes ranged from 2- to 10-fold lower on the microarray compared with rRT-PCR.

Given the implications of hypoxia-regulated PHD expression, we also analyzed the expression pattern of all three PHDs for their time and HIF1α-dependent expression by rRT-PCR. Wild-type and HIF1α –/– cells were left untreated or exposed to hypoxia (1% O_2) or cobalt (100 μM) for 0.25, 2, 8, 24, 48, and 72 h. PHD1 exhibited small but significant changes in expression at various times; however, these changes did not follow a pattern and did not appear HIF1α dependent (Fig. 8). PHD2 was significantly upregulated in a HIF1α-dependent manner in the wild-type cells as early as 15 min after exposure in both the hypoxia- and cobalt-treated cells. PHD3 showed a large increase (>11-fold) in the wild-type cells following hypoxia but not cobalt exposure (Fig. 8). The time course of this induction was also notably different from that of PHD2. The mechanism that controls the expression differences between the various PHDs has not been determined. These results indicate that the PHD genes are regulated by hypoxia in different ways. In addition, the identification of PHD2 and PHD3 as hypoxia-regulated genes suggests that the hypoxia signaling cascade may be partially controlled by feedback inhibition.

Finally, the microarray data suggest that loss of HIF1α leads to a downregulation of the basal levels of oxidative stress genes. The basal levels of expression of GST-μ, SOD1, SOD2, and catalase were verified by rRT-PCR. As seen in Figure 9, the basal levels of GST-μ, SOD1, and SOD2 were significantly repressed following loss of the HIF1α proteins. Catalase was not influenced in this comparison. The decreased level of expression of these protective enzymes may explain why HIF1α –/– cells are more susceptible to oxidative stress-induced damage (54).

PHD Effects on HIF-Mediated Transcription

The possibility that upregulation of the PHDs might lead to a feedback inhibition of HIF-mediated signal was tested in transient transfection experiments. Hep3B cells were transfected with an HRE-driven luciferase reporter and the various PHD expression plasmids. The cells were left at normoxia (20% O_2, ctrl) or hypoxia (1% O_2) for 18 h and analyzed for luciferase expression. PHD2 was capable of completely inhibiting HRE-mediated luciferase expression (Fig. 10). PHD3 was also capable of inhibiting this transactivation but to only 50% of controls (Fig. 10). Finally, hypoxia-mediated transcription displayed a 40% reduction in the presence of PHD1; however, this decrease was not significant. This supports the notion that these enzymes play a role in regulating the initial HIF signal and are also involved in attenuating the signal by feedback inhibition (1, 2,8).

DISCUSSION

Hypoxia-mediated signaling is critical to normal development and is strongly involved in several pathological conditions, including cancer and heart disease. Characterizing the upstream and downstream events following onset of hypoxia is critical to our ability to treat and understand these conditions. Recent publications have increased our understanding of the upstream signals involved in HIF stabilization and the role that hydroxylation plays in mediating the HIF:VHL interaction (8,16,18). However, our understanding of the downstream events is not as complete. For example, we do not know the events and proteins involved in translocating HIFs into the nucleus. In addition, we do not know what, if any, proteins are involved in controlling the ability of HIFs to interact with ARNT or ARNT2. Finally, we do not know the complete battery of hypoxia-regulated genes. The microarray is an excellent tool to address the latter knowledge gap. To this end we have used the NIA 15K gene set to identify novel hypoxia-regulated genes.

Our microarray experiments confirmed the expression of several known hypoxia-regulated genes, including glycolytic enzymes, proapoptotic genes, and a prolyl hydroxylase (Figs. 4 and 6, Table 2). These act as positive controls to confirm that our treatments, microarray experiments, and data processing are valid. In addition, it gave added confidence to the results that we observed for the novel hypoxia-regulated genes identified. To further validate the analysis, a comparison of the 49 gene identified in Figure 4 and Table 2 was made with a recently published report that used serial analysis of gene expression (SAGE) to analyze the effect of VHL and hypoxia on normal and tumor-derived renal cells (21). Given that the species and platforms are different, the extent of overlap will be underestimated. However, of the 49 genes identified as hypoxia responsive in this study, 12 were found to be hypoxia responsive in the SAGE study [supplemental data Table I and Fig. 3 of (21)]. This number is most likely higher due to the nature of SAGE and the genes represented on the microarray. For example, GLUT1 and GLUT2 were shown to be hypoxia responsive via SAGE while GLUT4 was found in this study (supplemental data Table I). In addition, GLUT1 and GLUT2 are not represented in the NIA 15K.

The microarray experiments confirmed that the

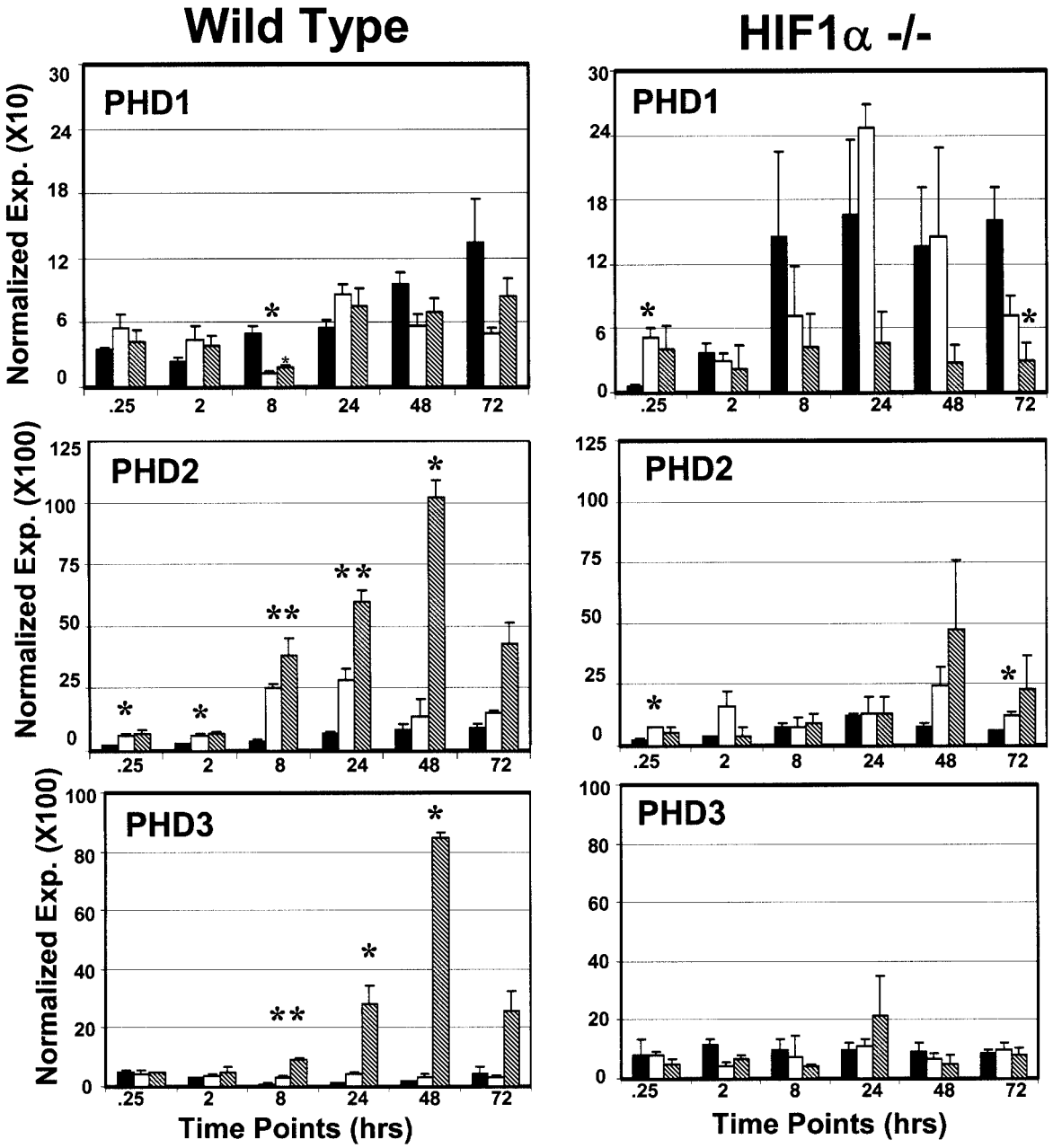

Figure 8. Time course analysis of the PHDs by rRT-PCR. The expression levels of the various PHDs were analyzed by rRT-PCR in wild-type (left) and HIF1α –/– (right) cells. Each bar represents an average value of six samples normalized to the expression level of the control gene and graphed as normalized expression. Black bars: untreated; white bars: 100 μM $CoCl_2$; hatched bars: 1% O_2 for 24 h. *$p < 0.05$ when compared with corresponding control.

hypoxic mimic, $CoCl_2$, increases a battery of genes similar to that of hypoxia. This overlap between expression patterns was only partial, suggesting differences in secondary signals or downstream signaling molecules. The exposure period was 24 h and each treatment may initiate other pathways and distinct secondary responses that will be observed at this time point. It should also be pointed out that the results observed in these studies with respect to the PHDs are in agreement with previously published reports; however, the time course and differences seen between cobalt and hypoxia treatments had not been previously described (6,8,34). Finally, the microarray experiments suggest that HIF1α is the primary cytoplasmic controller of hypoxia signaling in MEFs. This confirms recent reports suggesting HIF1α is the primary hypoxic-signaling protein (40).

The identification of PHD2 and PHD3 as hypoxia-

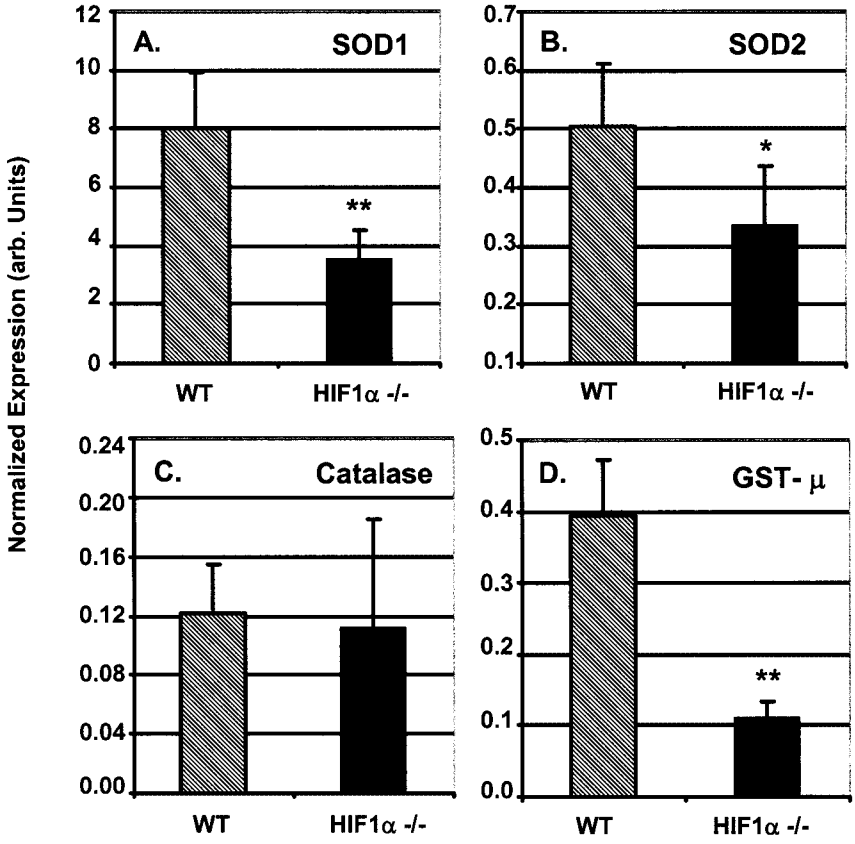

Figure 9. Analysis of basal levels of GST-μ, SOD1, SOD2, and catalase by rRT-PCR. The basal level of expression of genes involved in the cellular response to oxidative stress was analyzed by rRT-PCR. SOD1 (A), SOD2 (B), catalase (C), and GST-μ (D) were analyzed in untreated control cells to determine their relative levels of expression in wild-type (hatched bars) versus HIF1α –/– cells (solid bars). $^{**}p < 0.05$, $^{*}p < 0.1$.

regulated genes implies that HIF1α is prone to feedback inhibition (1). This feedback is not surprising when considering the implications of overstimulation of the hypoxia-signaling cascade. For example, the VHL protein is thought to be a tumor suppressor in part because of its ability to mediate the degradation of HIF (23). Once the VHL gene is mutated, this ability is lost and HIF signaling goes unabated, leading to the overproduction of a number of factors such as VEGF. This unchecked production of growth factors and other proteins may explain the hypervascularization of VHL –/– neoplasms (23). The control of the hypoxia-signaling cascade, both upstream and downstream, is therefore critical to normal cells and tissue homeostasis. We speculate that the feedback loop would limit the expression of the proapoptotic genes, thus giving the cell an alternative to programmed cell death. For example, the oxygen concentration of the cell at equilibrium may be "set" to limit damage due to small decreases in oxygen tension. Once these small fluctuations are encountered, the HIF protein is stabilized and the cell begins to transcribe the glyco-

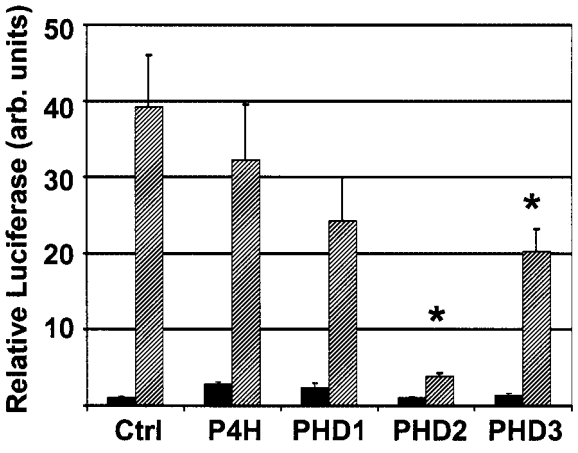

Figure 10. Transient transfection of Hep3b cells. Hep3b cells were transiently transfected with a HRE-driven reporter and one of the PHDs or an empty expression vector as a control. Transfected cells were left untreated (black bars) or exposed to hypoxia (1% O_2 (hatched bars) for 18 h. Luciferase levels were determined and normalized to cotransfected β-Gal activity and then to untreated control. $^{*}p < 0.05$ when compared with untreated sample.

lytic, proapoptotic, and PHD genes. As the level of the PHDs increases, the equilibrium between the available oxygen, PHDs, and HIF stabilization is shifted in favor of HIF hydroxylation. The increase in available PHDs would compensate for the small decrease in available oxygen. However, at larger decreases in oxygen tension, the cell would not be able to compensate by overproduction of the PHDs and the proapoptotic gene transcription would continue until the cell began its programmed cell death. One other feature of this feedback loop is the level of the individual PHDs within any given tissue and cell type. PHD1 was not upregulated by cobalt or hypoxia, so presumably it would not be able to participate in this type of regulation. Therefore, tissues that only express this isoform of the hydroxylase would not exhibit feedback inhibition. This idea of tissue-specific regulation and hydroxylase differences is supported by recent publications (6,34,38).

The role of HIF1α in maintaining proper cellular function during development and normal function is often neglected. The comparison of untreated wild-type and HIF1α –/– cells clearly showed that HIF1α has an important role in normal homeostasis. A battery of protective genes, such as SOD1 and SOD2, calmodulin (clones H3019D01 and H3021E08), and genes encoding metal binding proteins (metallothionein, clone 1-2031, and CRIP1 clone H3108G04) were shown to be negatively affected by the loss of the HIF1α protein (see Fig. 9 and supplemental data Table H). In addition, several genes were positively influenced by the loss of HIF1α. These results suggest that a basal level of HIF1α must be present to maintain transcriptional regulation for these genes. Alternatively, the loss of HIF1α may upset the signaling balance within the cell and these changes are the results.

In summary, these observations suggest a role for the PHDs in the feedback inhibition of the hypoxia-signaling cascade. The results also support the idea that cobalt and hypoxia exposure lead to the increase in the transcription of a number of gene families, including hydroxylases, glycolytic enzymes, and proapoptotic genes. The interplay between these families and the regulation of the downstream events may help to explain the role of hypoxia in mediating the damage following several pathological conditions, such as stroke and cardiovascular disease.

ACKNOWLEDGMENTS

The authors wish to thank Dr. Timothy Zacharewski and his laboratory for their careful reading of this manuscript and the extensive bio-informatics support. We would especially like to acknowledge Kirsten Fertuck, Lyle Burgoon, and Darrell Boverhof for their help in these endeavors.

REFERENCES

1. Berra, E.; Richard, D. E.; Gothie, E.; Pouyssegur, J. HIF-1-dependent transcriptional activity is required for oxygen-mediated HIF-1alpha degradation. FEBS Lett. 491:85–90; 2001.
2. Bruick, R. K.; McKnight, S. L. A conserved family of prolyl-4-hydroxylases that modify HIF. Science 294: 1337–1340; 2001.
3. Bruick, R. K. Expression of the gene encoding the proapoptotic Nip3 protein is induced by hypoxia. Proc. Natl. Acad. Sci. USA 97:9082–9087; 2000.
4. Bunn, H. F.; Poyton, R. O. Oxygen sensing and molecular adaptation to hypoxia. Phys. Rev. 76:839–885; 1996.
5. Choi, K. S.; Bae, M. K.; Jeong, J. W.; Moon, H. E.; Kim, K. W. Hypoxia-induced angiogenesis during carcinogenesis. J. Biochem. Mol. Biol. 36:120–127; 2003.
6. Cioffi, C. L.; Qin Liu, X.; Kosinski, P. A.; Garay, M.; Bowen, B. R. Differential regulation of HIF-1alpha prolyl-4-hydroxylase genes by hypoxia in human cardiovascular cells. Biochem. Biophys. Res. Commun. 303:947–953; 2003.
7. Dulak, J.; Jozkowicz, A.; Foresti, R.; Kasza, A.; Frick, M.; Huk, I.; Green, C. J.; Pachinger, O.; Weidinger, F.; Motterlini, R. Heme oxygenase activity modulates vascular endothelial growth factor synthesis in vascular smooth muscle cells. Antioxid. Redox Signal. 4:229–240; 2002.
8. Epstein, A. C.; Gleadle, J. M.; McNeill, L. A.; Hewitson, K. S.; O'Rourke, J.; Mole, D. R.; Mukherji, M.; Metzen, E.; Wilson, M. I.; Dhanda, A.; Tian, Y. M.; Masson, N.; Hamilton, D. L.; Jaakkola, P.; Barstead, R.; Hodgkin, J.; Maxwell, P. H.; Pugh, C. W.; Schofield, C. J.; Ratcliffe, P. J. *C. elegans* EGL-9 and mammalian homologs define a family of dioxygenases that regulate HIF by prolyl hydroxylation. Cell 107:43–54; 2001.
9. Falanga, V.; Zhou, L.; Yufit, T. Low oxygen tension stimulates collagen synthesis and COL1A1 transcription through the action of TGF-beta1. J. Cell Physiol. 191:42–50; 2002.
10. Fielden, M. R.; Halgren, R. G.; Dere, E.; Zacharewski, T. R. GP3: GenePix post-processing program for automated analysis of raw microarray data. Bioinformatics 18:771–773; 2002.
11. Forsythe, J. A.; Jiang, B. H.; Iyer, N. V.; Agani, F.; Leung, S. W.; Koos, R. D.; Semenza, G. L. Activation of vascular endothelial growth factor gene transcription

by hypoxia-inducible factor 1. Mol. Cell. Biol. 16: 4604–4613; 1996.
12. Gleadle, J. M.; Ratcliffe, P. J. Induction of hypoxia-inducible factor-1, erythropoietin, vascular endothelial growth factor, and glucose transporter-1 by hypoxia: Evidence against a regulatory role for Src kinase. Blood 89:503–509; 1997.
13. Grunstein, J.; Roberts, W. G.; Mathieu-Costello, O.; Hanahan, D.; Johnson, R. S. Tumor-derived expression of vascular endothelial growth factor is a critical factor in tumor expansion and vascular function. Cancer Res. 59:1592–1598; 1999.
14. Hewitson, K. S.; McNeill, L. A.; Riordan, M. V.; Tian, Y. M.; Bullock, A. N.; Welford, R. W.; Elkins, J. M.; Oldham, N. J.; Bhattacharya, S.; Gleadle, J. M.; Ratcliffe, P. J.; Pugh, C. W.; Schofield, C. J. Hypoxia-inducible factor (HIF) asparagine hydroxylase is identical to factor inhibiting HIF (FIH) and is related to the Cupin structural family. J. Biol. Chem. 277:26351–26355; 2002.
15. Hogenesch, J. B.; Chan, W. C.; Jackiw, V. H.; Brown, R. C.; Gu, Y.-Z.; Pray-Grant, M.; Perdew, G. H.; Bradfield, C. A. Characterization of a subset of the basic-helix-loop-helix-PAS superfamily that interact with components of the dioxin signaling pathway. J. Biol. Chem. 272:8581–8593; 1997.
16. Hon, W. C.; Wilson, M. I.; Harlos, K.; Claridge, T. D.; Schofield, C. J.; Pugh, C. W.; Maxwell, P. H.; Ratcliffe, P. J.; Stuart, D. I.; Jones, E. Y. Structural basis for the recognition of hydroxyproline in HIF-1 alpha by pVHL. Nature 417:975–978; 2002.
17. Huang, L. E.; Gu, J.; Schau, M.; Bunn, H. F. Regulation of hypoxia-inducible factor 1alpha is mediated by an O_2-dependent degradation domain via the ubiquitin-proteasome pathway. Proc. Natl. Acad. Sci. USA 95: 7987–7992; 1998.
18. Jaakkola, P.; Mole, D. R.; Tian, Y. M.; Wilson, M. I.; Gielbert, J.; Gaskell, S. J.; Kriegsheim, A.; Hebestreit, H. F.; Mukherji, M.; Schofield, C. J.; Maxwell, P. H.; Pugh, C. W.; Ratcliffe, P. J. Targeting of HIF-alpha to the von Hippel-Lindau ubiquitylation complex by O_2-regulated prolyl hydroxylation. Science 292:468–472; 2001.
19. Jeong, J. W.; Bae, M. K.; Ahn, M. Y.; Kim, S. H.; Sohn, T. K.; Bae, M. H.; Yoo, M. A.; Song, E. J.; Lee, K. J.; Kim, K. W. Regulation and destabilization of HIF-1alpha by ARD1-mediated acetylation. Cell 111: 709–720; 2002.
20. Jiang, B. H.; Semenza, G. L.; Bauer, C.; Marti, H. H. Hypoxia-inducible factor 1 levels vary exponentially over a physiologically relevant range of O_2 tension. Am. J. Physiol. 271:C1172–1180; 1996.
21. Jiang, Y.; Zhang, W.; Kondo, K.; Klco, J. M.; St Martin, T. B.; Dufault, M. R.; Madden, S. L.; Kaelin, W. G., Jr.; Nacht, M. Gene expression profiling in a renal cell carcinoma cell line: Dissecting VHL and hypoxia-dependent pathways. Mol. Cancer Res. 1:453–462; 2003.
22. Jung, Y.; Isaacs, J. S.; Lee, S.; Trepel, J.; Liu, Z. G.; Neckers, L. Hypoxia-inducible factor induction by tumour necrosis factor in normoxic cells requires receptor-interacting protein-dependent nuclear factor kappa B activation. Biochem. J. 370:1011–1017; 2003.
23. Kaelin, W. G.; Iliopoulos, O.; Lonergan, K. M.; Ohh, M. Functions of the von Hippel-Lindau tumour suppressor protein. J. Intern. Med. 243:535–539; 1998.
24. Kallio, P. J.; Okamoto, K.; S.; O. B.; Carrero, P.; Makino, Y.; Tanaka, H.; Poellinger, L. Signal transduction in hypoxic cells: Inducible nuclear translocation and recruitment of the CBP/p300 coactivator by the hypoxia-inducible factor-1alpha. EMBO J. 17: 6573–6586; 1998.
25. Kallio, P. J.; Wilson, W. J.; S.; O. B.; Makino, Y.; Poellinger, L. Regulation of the hypoxia-inducible transcription factor 1alpha by the ubiquitin-proteasome pathway. J. Biol. Chem. 274:6519–6525; 1999.
26. Kargul, G. J.; Dudekula, D. B.; Qian, Y.; Lim, M. K.; Jaradat, S. A.; Tanaka, T. S.; Carter, M. G.; Ko, M. S. Verification and initial annotation of the NIA mouse 15K cDNA clone set. Nat. Genet. 28:17–18; 2001.
27. Kerr, M. K.; Churchill, G. A. Statistical design and the analysis of gene expression microarray data. Genet Res. 77:123–128; 2001.
28. Kerr, M. K.; Martin, M.; Churchill, G. A. Analysis of variance for gene expression microarray data. J. Comput. Biol. 7:819–837; 2000.
29. Kothapalli, R.; Yoder, S. J.; Mane, S.; Loughran, T. P., Jr. Microarray results: How accurate are they? BMC Bioinformatics 3:22; 2002.
30. Krieg, M.; Marti, H. H.; Plate, K. H. Coexpression of erythropoietin and vascular endothelial growth factor in nervous system tumors associated with von Hippel-Lindau tumor suppressor gene loss of function. Blood 92:3388–3393; 1998.
31. Lahat, N.; Rahat, M. A.; Ballan, M.; Weiss-Cerem, L.; Engelmayer, M.; Bitterman, H. Hypoxia reduces CD80 expression on monocytes but enhances their LPS-stimulated TNF-alpha secretion. J. Leukoc. Biol. 74:197–205; 2003.
32. Lee, P. J.; Jiang, B. H.; Chin, B. Y.; Iyer, N. V.; Alam, J.; Semenza, G. L.; Choi, A. M. Hypoxia-inducible factor-1 mediates transcriptional activation of the heme oxygenase-1 gene in response to hypoxia. J. Biol. Chem. 272:5375–5381; 1997.
33. Li, H.; Ko, H. P.; Whitlock, J. P. Induction of phosphoglycerate kinase 1 gene expression by hypoxia. Roles of Arnt and HIF1alpha. J. Biol. Chem. 271: 21262–21267; 1996.
34. Lieb, M. E.; Menzies, K.; Moschella, M. C.; Ni, R.; Taubman, M. B. Mammalian EGLN genes have distinct patterns of mRNA expression and regulation. Biochem. Cell Biol. 80:421–426; 2002.
35. Mahon, P. C.; Hirota, K.; Semenza, G. L. FIH-1: A novel protein that interacts with HIF-1alpha and VHL to mediate repression of HIF-1 transcriptional activity. Genes Dev. 15:2675–2686; 2001.
36. Maltepe, E.; Simon, M. C. Oxygen, genes, and development: An analysis of the role of hypoxic gene regulation during murine vascular development. J. Mol. Med. 76:391–401; 1998.

37. Maxwell, P. H.; Dachs, G. U.; Gleadle, J. M.; Nicholls, L. G.; Harris, A. L.; Stratford, I. J.; Hankinson, O.; Pugh, C. W.; Ratcliffe, P. J. Hypoxia-inducible factor-1 modulates gene expression in solid tumors and influences both angiogenesis and tumor growth. Proc. Natl. Acad. Sci. USA 94:8104–8109; 1997.
38. Metzen, E.; Berchner-Pfannschmidt, U.; Stengel, P.; Marxsen, J. H.; Stolze, I.; Klinger, M.; Huang, W. Q.; Wotzlaw, C.; Hellwig-Burgel, T.; Jelkmann, W.; Acker, H.; Fandrey, J. Intracellular localisation of human HIF-1 alpha hydroxylases: Implications for oxygen sensing. J. Cell Sci. 116:1319–1326; 2003.
39. Murphy, B. J.; Andrews, G. K.; Bittel, D.; Discher, D. J.; McCue, J.; Green, C. J.; Yanovsky, M.; Giaccia, A.; Sutherland, R. M.; Laderoute, K. R.; Webster, K. A. Activation of metallothionein gene expression by hypoxia involves metal response elements and metal transcription factor-1. Cancer Res. 59:1315–1322; 1999.
40. Park, S. K.; Dadak, A. M.; Haase, V. H.; Fontana, L.; Giaccia, A. J.; Johnson, R. S. Hypoxia-induced gene expression occurs solely through the action of hypoxia-inducible factor 1alpha (HIF-1alpha): Role of cytoplasmic trapping of HIF-2alpha. Mol. Cell. Biol. 23: 4959–4971; 2003.
41. Poirier, F.; Chan, C. T.; Timmons, P. M.; Robertson, E. J.; Evans, M. J.; Rigby, P. W. The murine H19 gene is activated during embryonic stem cell differentiation in vitro and at the time of implantation in the developing embryo. Development 113:1105–1114; 1991.
42. Ryan, H. E.; Poloni, M.; McNulty, W.; Elson, D.; Gassmann, M.; Arbeit, J. M.; Johnson, R. S. Hypoxia-inducible factor-1alpha is a positive factor in solid tumor growth. Cancer Res. 60:4010–4015; 2000.
43. Ryan, H. E.; Lo, J.; Johnson, R. S. HIF-1 alpha is required for solid tumor formation and embryonic vascularization. EMBO J. 17:3005–3015; 1998.
44. Ryle, M. J.; Hausinger, R. H. Non-heme iron oxygenases. Curr. Opin. Chem. Biol. 6:193–201; 2002.
45. Sandner, P.; Wolf, K.; Bergmaier, U.; Gess, B.; Kurtz, A. Induction of VEGF and VEGF receptor gene expression by hypoxia: Divergent regulation in vivo and in vitro. Kidney Int. 51:448–453; 1997.
46. Semenza, G. L. Regulation of mammalian O_2 homeostasis by hypoxia-inducible factor 1. Annu. Rev. Cell Dev. Biol. 15:551–578; 1999.
47. Semenza, G. L.; Roth, P. H.; Fang, H. M.; Wang, G. L. Transcriptional regulation of genes encoding glycolytic enzymes by hypoxia-inducible factor 1. J. Biol. Chem. 269:23757–23763; 1994.
48. Sowter, H. M.; Ratcliffe, P. J.; Watson, P.; Greenberg, A. H.; Harris, A. L. HIF-1-dependent regulation of hypoxic induction of the cell death factors BNIP3 and NIX in human tumors. Cancer Res. 61:6669–6673; 2001.
49. Tajima, R.; Kawaguchi, N.; Horino, Y.; Takahashi, Y.; Toriyama, K.; Inou, K.; Torii, S.; Kitagawa, Y. Hypoxic enhancement of type IV collagen secretion accelerates adipose conversion of 3T3-L1 fibroblasts. Biochim. Biophys. Acta 1540:179–187; 2001.
50. Takahata, S.; Sogawa, K.; Kobayashi, A.; Ema, M.; Mimura, J.; Ozaki, N.; Fujii-Kuriyama, Y. Transcriptionally active heterodimer formation of an Arnt-like PAS protein, Arnt3, with HIF-1a, HLF, and clock. Biochem. Biophys. Res. Commun. 248:789–794; 1998.
51. Takahashi, Y.; Takahashi, S.; Shiga, Y.; Yoshimi, T.; Miura, T. Hypoxic induction of prolyl 4-hydroxylase alpha (I) in cultured cells. J. Biol. Chem. 275:14139–14146; 2000.
52. Tanaka, T. S.; Jaradat, S. A.; Lim, M. K.; Kargul, G. J.; Wang, X.; Grahovac, M. J.; Pantano, S.; Sano, Y.; Piao, Y.; Nagaraja, R.; Doi, H.; Wood, W. H., 3rd; Becker, K. G.; Ko, M. S. Genome-wide expression profiling of mid-gestation placenta and embryo using a 15,000 mouse developmental cDNA microarray. Proc. Natl. Acad. Sci. USA 97:9127–9132; 2000.
53. Vaupel, P.; Schlenger, K.; Knoop, C.; Hockel, M. Oxygenation of human tumors: Evaluation of tissue oxygen distribution in breast cancers by computerized O_2 tension measurements. Cancer Res. 51:3316–3322; 1991.
54. Williams, K. J.; Telfer, B. A.; Airley, R. E.; Peters, H. P.; Sheridan, M. R.; van der Kogel, A. J.; Harris, A. L.; Stratford, I. J. A protective role for HIF-1 in response to redox manipulation and glucose deprivation: Implications for tumorigenesis. Oncogene 21: 282–290; 2002.
55. Wykoff, C. C.; Pugh, C. W.; Maxwell, P. H.; Harris, A. L.; Ratcliffe, P. J. Identification of novel hypoxia dependent and independent target genes of the von Hippel-Lindau (VHL) tumour suppressor by mRNA differential expression profiling. Oncogene 19:6297–6305; 2000.
56. Yet, S. F.; Melo, L. G.; Layne, M. D.; Perrella, M. A. Heme oxygenase 1 in regulation of inflammation and oxidative damage. Methods Enzymol. 353:163–176; 2002.
57. Zien, A.; Aigner, T.; Zimmer, R.; Lengauer, T. Centralization: A new method for the normalization of gene expression data. Bioinformatics 17:S323–331; 2001.